Mat. Res. Soc. Symp. Proc. Vol. 708 © 2002 Materials Research Society

Optical Spectroscopic Studies of a Soluble Fluorene-Based Conjugated Polymer: A Hydrostatic Pressure and Temperature Study

S. Guha[1], J.D. Rice[1], C. M. Martin[2], W. Graupner[3], M. Chandrasekhar[2], H.R. Chandrasekhar[2] and U. Scherf[4]
[1] Dept. of Physics, Astronomy and Materials Science, Southwest Missouri State University, Springfield MO 65804 (USA).
[2] Dept. of Physics and Astronomy, University of Missouri, Columbia MO 65211 (USA).
[3] Dept of Physics and Astronomy, Virginia Tech, Blacksburg, VA 24061; Present address: Austriamicrosystems, AG; Schloss Premstaetten, A 8141 Austria.
[4] Institut für Physikalische und Theoretische Chemie, Universitaet Potsdam, Germany.

ABSTRACT

Spectroscopic properties of conjugated molecules/polymers have varying degrees of sensitivity to backbone conformation. Optical studies are presented as a function of temperature and hydrostatic pressure, using photoluminescence and Raman scattering from two polymers with distinct differences in their backbone conformation, namely, polyfluorene (PF) and ladder type poly(para-phenylene)(m-LPPP). In contrast to the photoluminescence (PL) vibronics in m-LPPP, the 0-0 PL vibronic peak in PF shows a red-shift with increasing temperatures. Pressure studies reveal that the PL spectrum of PF red-shifts and broadens with increasing pressures. The phonon lines in PF show an antiresonance effect at higher pressures indicating a strong electron-phonon interaction.

INTRODUCTION

Conjugated organic molecules such as short-chain oligomers and longer-chain polymers are very promising active materials for low-cost, large-area optoelectronic and photonic devices. The ability of these materials to transport charge (holes or electrons) due to the π-orbital overlap of neighboring molecules defines their semiconducting and conducting properties. Devices such as organic light-emitting diodes (OLEDs), transistors, and photodiodes are currently attracting much attention [1]. Blue electroluminescent materials are of particular interest for organic displays since blue light can be converted into red and green quite easily by color-changing media (fluorescent dyes). Both polyfluorene (PF) and the methyl substituted ladder-type poly(para-phenylene) (m-LPPP) are of technological importance due to their strong blue luminescence. PF based conjugated polymers show the highest photoluminescence (PL) quantum efficiency (55%) compared to other conjugated polymers/molecules in solid state [2] and also have a high hole mobility at room temperature [3].

Figure 1 shows the chemical structure of m-LPPP and PF (poly 9,9-bis-2-ethylhexyfluorene-2,7-diyl). The backbone of m-LPPP is planar and shows no torsional degree of freedom between the neighboring phenyl rings due to the methyl bridges. The planar backbone in m-LPPP results in a high intrachain order and low defect concentration. This is attributed to its synthesis, which selectively forms only certain bonds and hence reduces the number of defects. PF, on the other hand, is planar within a single monomer unit but shows a torsional degree of freedom between two monomer units.

EXPERIMENTAL

PL spectra were measured from films of m-LPPP and PF, prepared by spin coating on a glass slide from toluene solution. The films were dried at room temperature. The PL spectra were excited using the 351.1 nm line of an Ar^+ laser. The luminescence radiation was analyzed with a SPEX 0.85 m double monochromator equipped with a cooled GaAs photomultiplier tube and standard photon counting electronics. For low temperature measurements a closed cycle refrigerator was employed. Raman measurements were carried out in a back-scattering configuration, using the 647nm line of a Kr^+ laser. The laser power was 10 mW with a spot size of 50 microns. The scattered light was detected with a SPEX triple monochromator equipped with a CCD array detector and a holographic supernotch filter. Pressure studies were conducted in a Merrill-Bassett type diamond anvil cell (DAC) with cryogenically loaded argon as the pressure medium. PF in its powdered form was used for the pressure studies. PL under pressure was measured with an Ocean Optics 2000 spectrometer with 25-micron slits. Pressure was measured via the luminescence of a ruby chip.

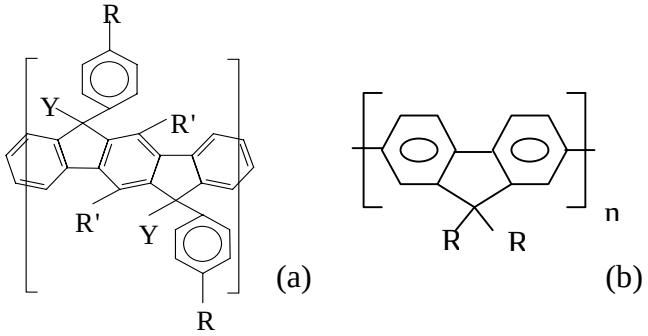

Figure 1. Chemical structure of (a) m-LPPP and (b) PF (R =ethyl hexyl).

PL RESULTS

Comparison of PL emission (m-LPPP and PF)

PF films show different crystalline phases on varying the growth conditions. Comparing the PL spectrum of PF in Figure 2 with other work shows that our samples are in the glassy phase [4,5]. The PL emission from PF is blue-shifted in comparison with m-LPPP (Fig.2). A vibronic progression is seen in the PL emission of both materials, which indicates a coupling of the backbone carbon-carbon stretch vibration to electronic transitions. The vibronic spacing in both materials lies between 1300-1400 cm^{-1}. The vibronic peaks result from the non-zero overlap of different vibronic wavefunctions of the electronic ground and excited states. The emissive transition highest in energy is called the 0-0 transition which takes place between the zeroth vibronic level in the excited state and the zeroth vibronic level in the ground state. The 0-1 transition involves the creation of one phonon.

In the adiabatic picture, vibronic progression in the electronic spectra implies that the ground and excited state equilibrium structures are displaced relative to one another in configuration-space. The spectral intensity is approximated by the superposition of transitions between the vibrational frequencies of the ground- and the excited electronic states. The probability of the 0^{th} vibronic ground state to the n^{th} vibronic excited state is given by

$$I_{0\to n} = \frac{e^{-S} S^n}{n!}, \qquad (1)$$

where S, the Huang-Rhys factor, is given by $S = M\omega / 2\hbar(\Delta)^2$ [6]. Here ω is the vibrational frequency, M is the reduced mass of the harmonic oscillator that couples to the electronic transition and Δ is the displacement of the potential curve between the ground and excited electronic states. The Huang–Rhys factor therefore corresponds to the average number of phonons that are involved when the excited molecule relaxes from its ground state configuration to the new equilibrium configuration in the excited state (after the absorption of a photon) and Sħω is the relaxation energy. If we assume that ω is the same for ground and excited states and that the potentials are perfectly parabolic, S can be determined from the fractional intensity of the vibronic peaks. In particular, it is equal to $I_{0\to 1} + 2\times I_{0\to 2}$ divided by the total intensity. $I_{0\to 1}$ and $I_{0\to 2}$ refer to the intensity of the zeroth vibrational level excited state to the first and second vibrational level of the ground state, respectively. Here we assume that the transition matrix elements are the same for all vibronics and we neglect all vibronics above 0-2.

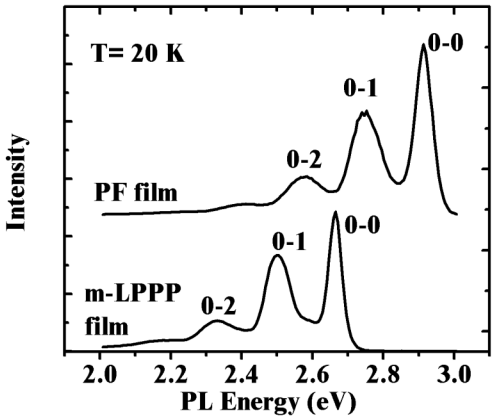

Figure 2. PL spectra from a PF film and m-LPPP film at 20K.

From an analysis of the PL data we find that S = 0.7 for both m-LPPP and PF at 20K. At lower temperatures one would expect the freezing out of the molecular torsions in non-planar molecules. In non-planar molecules the torsional frequencies usually couple to the π-π* excitation resulting in a broadening of the absorption spectrum and a higher Huang-Rhys factor [7]. It is observed that in non-planar *para* hexaphenyl (PHP) the value of S is higher (~2) [8]. Our results here indicate that the frequency of the torsional motion between the monomer units in PF does not contribute significantly to the electronic states since the value of S for PF is the same as in m-LPPP, which is planar.

PL vibronics as a function of temperature

With increasing temperature, not only do the PL vibronics shift but the relative strengths of the vibronic transitions change as well. The relative strength of the 0-0 transition decreases with increasing temperatures compared to the 0-1 and 0-2, both in m-LPPP and PF. This indicates that the Huang-Rhys factor itself increases with increasing temperature as a result of decreased conjugation and exciton localization [9]. Increasing temperature therefore results in a higher coupling of the C-C vibrations to the electronic states. The apparent change in vibronic intensities is partly due to the stronger contribution from lower lying emission as well.

Figure 3 shows the PL vibronics as a function of temperature in m-LPPP and PF. The 0-0 and 0-1 vibronics in m-LPPP blue-shift with increasing temperatures. The 0-2 peak in m-LPPP also shows a similar behavior. This trend is seen in other conjugated polymers like MEH-PPV [10] and PPV [9]. The PL transition energies in PF show a unique dependence on temperature.

The 0-0 peak energy red-shifts with increasing temperatures while the 0-1 peak shows a blue-shift with increasing temperatures. Shorter conjugated molecules show the reverse trend compared to m-LPPP. The PL vibronics in PHP show a red-shift with increasing temperatures [8], similar to the shift of the interband transition energies in inorganic semiconductors [11,12].

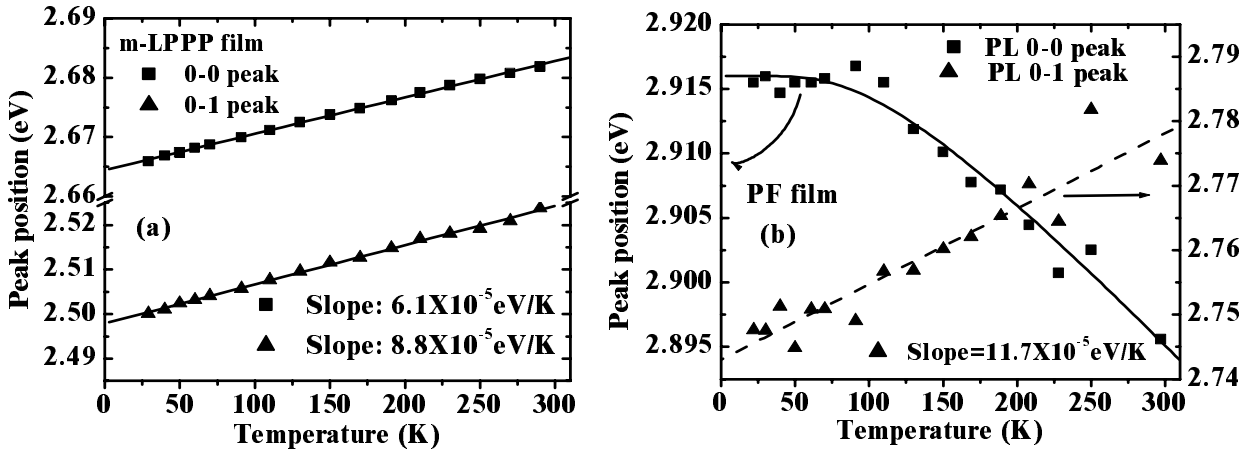

Figure 3. (a) Peak position of the 0-0 and 0-1 PL vibronics in m-LPPP as a function of temperature. (b) Peak position of the 0-0 and 0-1 PL vibronics in PF as a function of temperature.

The electronic energies in bulk inorganic semiconductors display temperature dependence mainly due to thermal expansion and renormalization of band energies by electron-phonon interactions. The temperature dependence of the interband transitions can be described with an expression in which the energy thresholds decrease proportional to the Bose-Einstein statistical factors for phonon emission plus absorption [11]. By fitting the 0-0 PL peak of PF (shown as a bold line in Fig. 3(b)) with Eq. (2) of Ref. [12] we obtain an average phonon temperature of 323 K in PF.

PL emission as a function of pressure

Figure 4 shows the PL spectra of PF powder for five pressure values. The PL line shape changes dramatically beyond 20 kbar, beyond which the individual vibronics are no longer discernable. The entire PL emission exhibits a red-shift with increasing pressures. By fitting the PL emission with a single Gaussian peak (beyond 25 kbar), the pressure coefficient is found to be –1.86± 0.3 meV/kbar. In m-LPPP the individual vibronics are found to shift (~-2.5 meV/kbar) with a higher rate but the overall PL emission shows a slower shift with increasing

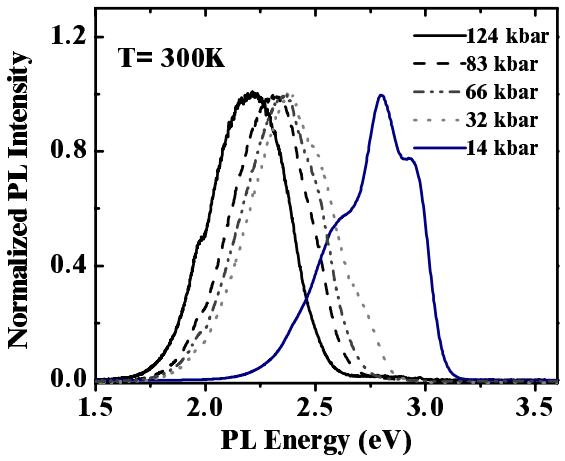

Figure 4. PL spectra of PF at 124 kbar, 83 kbar, 66 kbar, 32 kbar and 14 kbar (left to right).

pressure [13]. Also, in m-LPPP there is a broadening of the PL vibronics observed with increasing pressure but the individual vibronics can be distinguished up to 80 kbar. The red-shift and broadening of the PL spectrum with increasing pressures in conjugated molecules can be understood as being due to a change in chain conformation or crystallization arising from a stronger overlap of π-electron wavefunctions [14].

RAMAN SCATTERING RESULTS

Figure 5 (a) compares the Raman spectrum of m-LPPP and PF. The spectra were measured at ambient pressure. The Raman peaks around 1130 cm^{-1} are from the C-H bend modes. The peaks in the 1300-1400 cm^{-1} region are from the backbone C-C stretch modes. The Raman peaks in the 1600 cm^{-1} region are from the intra-ring C-C stretch mode. Since PF has a torsional degree of freedom between the monomer units one would expect C-C stretch modes both from the monomer and from the bonds connecting the two monomers. At lower temperatures the molecule should be more non-planar compared to that at room temperature where the average conformation is planar. Raman intensities show subtle changes when conjugated molecules change from a planar to non-planar conformation [13].

Our temperature dependent Raman studies of PF indicate that the 1417 cm^{-1} mode is from the C-C stretch within the monomer whereas the 1342 cm^{-1} and the 1290 cm^{-1} modes are from phenyl rings connecting the monomer units. In planar m-LPPP the backbone C-C stretch mode appears at ~1320 cm^{-1}. It is interesting to note that the 1580 cm^{-1} and 1607 cm^{-1} modes observed in this region reverse their intensity in these two materials.

Figure 5 (b) shows the Raman spectra of PF for different values of pressure. The break in the *x*-axis denotes the region where the diamond peak from the DAC is observed. The phonon lines exhibit an antiresonance (not shown in the figure) effect at higher pressures, which is most likely due a high electron-phonon interaction between the Raman phonons and the (real) PL transitions. Upon lowering the pressure, the 1600 cm^{-1} mode is observable at ~50 kbar and the lower energy

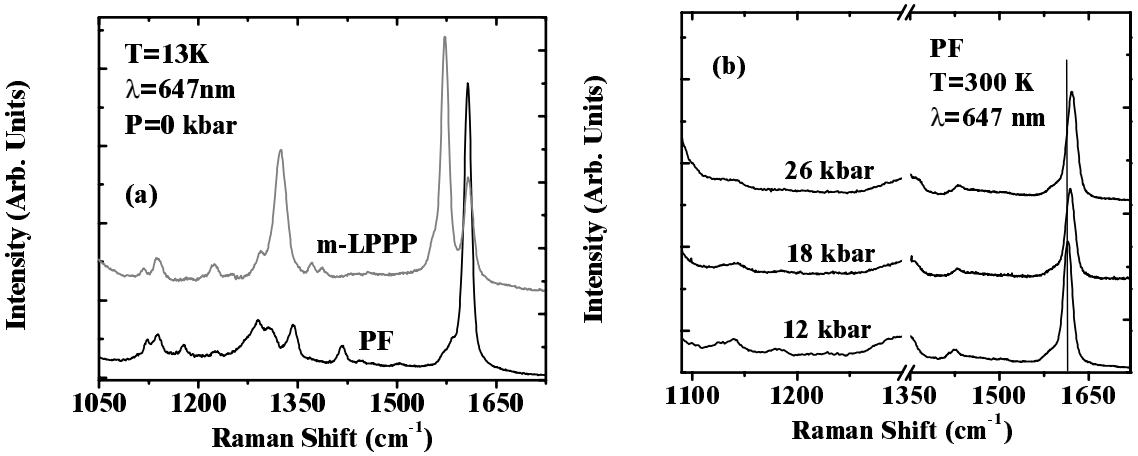

Figure 5. (a) Raman spectra of m-LPPP and PF at ambient pressure. (b) Raman spectra of PF for different values of hydrostatic pressure.

Raman peaks re-appear at even lower values of pressure. An analysis of data shown in Fig. 5(b) indicates that the Raman frequencies increase linearly with pressure, an effect that is completely reversible.

CONCLUSIONS

Optical studies from two distinct polymers with varying degrees of backbone conformation reveal that their photoluminescence emission and the Raman spectra change considerably as a function of temperature and hydrostatic pressure. A detailed optical study of PF under hydrostatic pressure is currently in progress to fully understand the behavior of the electron-phonon interaction in this system under enhanced intermolecular interaction.

ACKNOWLEDGEMENTS

Work at SMSU was partly funded by an award from Research Corporation #CC5332 and the Petroleum Research Fund #35735-GB5. SG would like to acknowledge the summer faculty fellowship from SMSU. Work at MU was funded by the University of Missouri research board.

REFERENCES

1. For a review see "*Organic electronics: introduction*", J.M. Shaw and P.F. Seidler, IBM J. Res. & Dev. **45**, 3 (2001); Handbook of Conducting Polymers, edited by T.A. Skotheim, R.L. Elsenbaumer and J.R. Reynolds, Marcel Dekker, Inc. (1997).
2. A.W. Grice, D.D. C. Bradley, M.T. Bernius, M. Inbasekaran, W.W.Wu, and E.P. Woo, Appl. Phys. Lett. **73**, 629 (1998).
3. M. Redecker, D.D.C. Bradley, M. Inbasekaran, and E.P. Woo, Appl. Phys. Lett. **73**, 1565 (1998).
4. A.J. Cadby, P.A. Lane, H. Mellor, S.J. Martin, M. Grell, C. Giebeler, D.D.C. Bradley, M.Wohlgenannt, C. An and Z.V. Vardeny, Phys. Rev. B **62**, 15604 (2000).
5. M. Ariu, D.G. Lidzey, and D.D.C. Bradley, Synth. Met. **111-112**, 607 (2000).
6. H. Bassler, and B. Schweitzer, Acc. Chem. Res. **32**, 173 (1999).
7. S. Karabunarliev, R.R. Bitner, and M. Baumgarten, J. Chem. Phys. **114**, 5863 (2001).
8. S. Guha, S. Yang, W. Graupner, M. Chandrasekhar, H.R. Chandrasekhar (unpublished)
9. S-H Lim, T.G. Bjorklund, and C.J. Bardeen, Chem. Phys. Lett. **342**, 555 (2001).
10. A.K. Sheridan, J.M. Lupton, I.D.W Samuel, and D.D.C. Bradley, Chem. Phys. Lett. **322**, 51 (2001).
11. P. Lautenschlager, M. Garriga, S. Logothetidid, and M. Cardona, Phys. Rev. B **35**, 9174 (1987).
12. S. Guha, Q. Cai, M. Chandrasekhar, H.R. Chandrasekhar, H. Kim, A.D. Alvarenga, R. Vogelgesang, and A.K. Ramdas, Phys. Rev. B **58**, 7222 (1998).
13. S. Guha, W. Graupner, S. Yang, M. Chandrasekhar, H.R. Chandrasekhar, and G. Leising, Phys. Stat. Sol.(B) **211**, 177 (1999); S. Guha, W. Graupner, R. Resel, M. Chandrasekhar, H.R. Chandrasekhar, R. Glaser, and G. Leising, Phys. Rev. Lett. **82**, 3625 (1999).
14. S. Yang, W. Graupner, S. Guha, P. Puschnig, C. Martin, H. R. Chandrasekhar, M. Chandrasekhar, G. Leising, C. Ambrosch-Draxl, Phys. Rev. Lett. **85**, 2388 (2000).